HIGH RESOLUTION MEASUREMENTS OF ENERGY LOSS DISTRIBUTION OF LIGHT IONS WITH ~100 KEV TRANSMITTED THROUGH CARBON FILMS

Noriaki Matsunami
Energy Engineering and Science, School of Engineering,
Nagoya University, Furo-cho, Chikusa-ku, Nagoya 464-01, Japan

Abstract

Energy loss distribution(ELD) of H^+, He^+ and H_2^+ with ~100 keV transmitted through carbon films has been measured with a high resolution (~30 eV) in order to investigate details of the electronic energy loss process. The results are as follows.

(1) No peak corresponding to plasmon excitation was observed.

(2) The zero energy loss peak was detected and the inelastic mean free path(IMFP) was deduced as 0,6 and 0,9 nm for 100 keV H^+ and He^+, respectively.

(3) The main ELD deviates significantly from the Gaussian and agrees well with the ELD of simulation (Vavilov distribution and etc.), including non uniformity of films.

(4) The ratio of the full-width at the half maximum of H_2^+ over H+ was varied from 1,3-1,6 and these deviate from 1,41 of the independentparticle model, indicating that the vicinage effect on the straggling differs from that on the energy loss.

1 Introduction

The electronic stopping powers of swift ions in solids are well documented as in ref. [1]. However, the details of the electronic energy loss processes have not been fully established yet. For example, energy loss peak due to plasmon excitation (one of the fundamental excitations) has not been observed for ions [2], in contrast to the electron impact [3]. Furthermore, there is scarce knowledge of the the inelastic mean free path (IMFP) for swift ions [4], again in contrast with electrons [3,5]. Here, the IMFP is a measure of the interaction strength or total cross section of the electronic excitation and ionization, and is also one of the fundamental quantities for the swift ions interacting with electrons in solids.

This paper reports the energy loss distribution (ELD) that has been measured for H^+ and He^+ ions with ~ 100 keV in carbon films by means of high-resolution ion energy loss spectroscopy (HRIELS) with a resolution of ~30 eV, in order to search for the plasmon peak, zero energy loss peak which yields the IMFP, details of main ELD (e.g., deviation from Gaussian distribution, straggling etc.) and ELD of H_2^+. The results and points to be discussed are the followings. No plasmon peak was observed for 100 keV H^+. A crude estimation was made for the intensity of the plasmon peak and compared with the experimental results. The zero energy loss peak was detected and the inelastic mean free path (IMFP) was derived as 0,6 and 0,9 nm for 100 keV H^+ and He^+, after correcting the pin-hole effects inferred from the H_2^+ transmission efficiency. The present IMFP values are compared with the calculated values. The experimental ELD is compared in details with the simulated ELD including the non-uniformity of films. The ELD of H_2^+ is also presented and discussed in terms of the independentparticle model.

2 Experimental

2.1 High Resolution Energy Loss Spectrometer(HRIELS)

The details of the experimental set up of HRIELS, as shown in Fig. I, have been reported elsewhere [2,6] and a brief description is reproduced here. Ions are generated with a hollow cathode ion source and accelerated to the voltage of V_a. After analyzed by a magnet and deflected by 12° with an electrostatic deflector, ions impinge on a carbon film supported on a copper mesh.

Ions transmitted through carbon films are led into a deceleration tube through a circular aperture with an acceptance angle of 1.1 degrees and decelerated by $V_d=V_a-V_o$ to the final energy Ef=l keV, where V_o is the offset voltage. Then only ions with the energy of Ef are able to pass through an electrostatic analyzer and finally detected by a secondary electron multiplier. The energy loss ΔE is given by,

$$\Delta E=qVo - Ef, \qquad (I)$$

where q is the charge of the ion. In the present method, ions can be detected only when q after transmission through a film is the same as q of incidence. The energy loss spectrum is obtained by varying the offset voltage. Retardation of ions is a key to achieve high energy resolution .

The beam size was ~1 mm^2 and the beam current was 0,1-1 nA. The vacuum of the sample chamber was ~1 $^{-7}$ Torr. The carbon film/Cu mesh has capability of linear motion and the energy loss with or without a carbon film can be measured without changing the experimental conditions. The resolution was measured as ~30 eV for 100 keV H^+ and He^+, and ~ 60 eV for 100 keV H_2^+.

2.2 Carbon films

Carbon films were prepared by the arc discharge method. Impurities in the carbon film which was placed on Be substrates were examined by ion beam spectroscopy [7]. The 2 MeV He^+ RBS (Rutherford backscattering spectroscopy) shows less than a few % of heavier elements than carbon. The 1,5 MeV He^+ ERD (elastic recoil detection) shows ~10 % H. For 100 keV H^+ and He^+, this amount of H contributes to the stopping power by ~3 % and 2 %, respectively [1]. Herein, the Bragg additive rule is assumed. Replacement of C-C bonds by C-H bonds results in increase of the stopping power by ~5% [8], though a simple replacement of 10 % C by H leads to ~7 % decrease of the stopping power. Moreover, H-release by ion beam was observed. After all, the contribution of H to the stopping power is insignificant.

2.3 Film Thickness Determination

The film thickness ℓ was determined by the mean energy loss (as indicated by the vertical arrows in Fig. 3) with the stopping cross section Se in ref.[1] (Se=13,8, 13,6, 25,2x10^{-15} $eVcm^2$ for 100 keV H^+, 120 keV H^+ and 100 keV He^+) and density p=2,2 g/cm^3. This density was chosen, considering the ion beam induced modification of carbon films (graphitization) during measurements [9-11] and the density dependence of the plasmon peak [12]. The plasmon energy of C film used in this study was observed at 24 ± 1 eV by the energy loss of 100-200 keV electrons, as shown in Fig.2. By graphitization, the film density ρ varies from ~2 to 2,2 g/cm^3 [12]. Correspondingly, the electronic stopping cross sections for 100 keV H^+ and He^+ are estimated to be enhanced by 10-20 % [8,11]. Taking these effects into account, the overall error of the film thickness is estimated as ± 10%. The film thickness fluctuation was estimated as 10-20 % and the details will be discussed later.

3 RESULTS AND DISCUSSION

3.1 Plamon Excitation Peak

Typical energy loss spectra are shown in Fig. 3(a) and (b) for 100 and 120 keV H^+ transmitted through a carbon film. The main energy loss peak is seen at around 1 keV. The main energy loss peak can be fitted by the asymmetric Gaussian [13] as indicated by the solid line,

$$Fg(\Delta E)=\exp\{-\log2(\Delta E-\Delta Ep)^2/W2\},$$
$$W=W_1 \text{ for } \Delta E<\Delta E_p \text{ and } W=W_2 \text{ for } \Delta E>\Delta E_p. \qquad (2)$$

Here ΔE_p is the most probable energy loss or the peak energy loss and W_1 and W_2 are the half width at half maximum (HWHM) of the lower and higher energy loss sides.

No peak due to plasmon excitation around 25 eV was seen, in contrast to the electron impact (see Fig.2). A crude estimate of the plasmon peak intensity will be discussed in §3.3. Surprisingly, a peak was seen at $\Delta E = \sim 210$ eV. The origin of this peak has not been identified yet [14].

3.2 Inelastic Mean Free Path(IMFP)

Careful measurements were made to clarify the zero energy loss peak [4] which is unclear in Fig. I. A problem to obtain the true zero energy loss peak, from which the IMFP is derived, is the presence of pinholes in the films. To reduce the pinhole effect, the zero energy loss peak for H_2^+ impact was subtracted from that of H^+ impact, since the recombination mechanism for H_2^+ transmission is dominant in this study and hence the zero energy loss peak intensity of H_2^+ is due to pinholes, assuming the same transmission efficiency of H_2^+ and H^+.

This assumption was verified by the comparison of the transmission efficiency of H_2^+ with those in literature [15].

Fig. 4 shows the main and zero energy loss peaks. The IMFP λ_0 is given by

$$\exp(-\ell/\lambda_0) = I_0/(I_0 + I_m), \qquad (2)$$

where I_0 and I_m are the zero and main energy loss peak intensities, respectively. For 100 keV H^+ and He^+, λ_0 are obtained as 0,6 and 0,9 nm. In Fig. 5, the results are compared with the calculated values [4] after refs. [17-19] and also with the experimental values for e^- [20-22]. The present IMFP values are somewhat larger than the calculated values.

Next, the experimental stopping power (lst moment of ELD) is compared with the theoretical values. Typical values of the calculated IMFP and stopping powers with various dielectric functions [17-19] are listed in Table I (see ref. [4] for the details of calculation). In this calculation, contribution of K-shell to the stopping powers (0,5; 1,3 and 5,6 0/0 for 25, 100 and 400 keV H^+ [23]) are discarded. Also included are the semi-empirical stopping powers [1]. Notice also that no dielectric function satisfies the IMFP and stopping power at the same time.

3.3 Estimate of the Plasmon Peak Intensity

Now, a crude estimate was made for the plasmon peak intensity. The mean free path λ_{eh} of the e-h (electron-hole) pair excitation is given by

$$\lambda_{eh} = \langle\Delta E\rangle eh/(dE/dx)eh, \qquad (3)$$

where, $\langle\Delta E\rangle eh$ and $(dE/dx)eh$ are the average energy and the stopping power for the e-h pair excitation. The mean free path λ_p of the plasmon excitation is estimated using a equation [3]

$$\lambda_p = \hbar\omega_p \Big/ \left\{ \left(e \bullet \omega_p / V \right)^2 \log\left(V_F / V \right) \right\}. \qquad (4)$$

Here $\hbar\omega_p$ is plasmon energy (24 eV), e is the proton charge, V the ion velocity and V_f the Fermi velocity (2,73x10^8cm/s). For 100 keV H^+ (V=4,38x10^8cm/s), λp and the stopping power due to plasmon excitation ($(dE/dx)p = \hbar\omega_p/\lambda_p$) are evaluated as 0,51 nm and 47 eV/nm.

The value $(dE/dx)_{eh}$ is obtained as 105 eV/nm by subtracting $(dE/dx)_p$ from the experimental (dE/dx) value (152 eV/nm) and λ_{eh} as 0,095-0,19 nm, for $\langle\Delta E\rangle_{eh}$ =10-20 eV. Herein, a small contribution from K-shell electrons is neglected. The IMFP λ_0 is taken as 0,6 nm (see § 3,2). Next, we adopt the slicing method to obtain the energy loss spectrum and let n be the effective number of layers in the film(the thickness of each layer= ℓ/n, with the film thickness ℓ). One gets the probability P_i for each excitation or no excitation

$$Pi = (1/\lambda i)/(1/\lambda_{eh} + 1/\lambda_p + 1/\lambda_o) \quad i = eh,\ p \text{ or } o. \qquad (5)$$

One obtains Peh=0.74-0.59, Pp=0.14-0.22 and Po=0.12-0.19, for $\langle\Delta E\rangle eh$ =10-20 eV. Assuming independence between excitations and discarding the plasmon contribution, the normalized intensity of the zero energy loss peak f_o (see §3.2) is thus written as,

$$f_o=I_o/(I_o+I_m)=P_o^n \qquad (6)$$

For 100 keV H^+ in 6,6 nm C film, $f_o=\exp(-6,6/0,6)=1,7x10^{-5}$, thus n= 5,2-6,6. Hence, we have the plasmon peak intensity $f_p=P_p{\cdot}P_o^{n-1}$ = ~$2x10^{-5}$, which is comparable with the zero energy loss peak intensity and should be observed, if the values used above are reasonable. However, some parameters used above are uncertain, and further theoretical and experimental investigations are to be done.

3.4 Energy Loss Straggling

The energy loss straggling Ω^2, which is defined as the second moment of the energy loss distribution, is also one of the fundamental quantities of ions interacting with electrons in solids. For Gaussian or asymmetric-Gaussian energy loss distribution, the variance $(W_1+W_2)^2/5.545$, where W_1+W_2=FWHM (full width at half maximum of ELD), is expressed by [24,25]

$$(W_1 +W_2)^2/5 .545=\Omega^2 N \ell + \left(\delta\ell S_e N\right)^2 \qquad (7)$$

Here N is the atomic density and S_e the electronic stopping cross section. The second term arises from the contribution $(\delta\ell)^2$ or the variance of the film thickness fluctuation. It appears that the experimental data fit well to eq. (7) with a constant $\delta\ell$ [13]. The straggling in Bohr units or Ω^2 / Ω_B^2 are obtained as 0,6 and 0,34 for H^+ andHe^+ at 100 keV, in reasonable agreement with theoretical values of 0,79 [26] for H^+, and 0,25 [27] and 0,44 [26] for He^+ (see ref. [13]).

The thickness fluctuation $\delta\ell$ is also obtained as ~2 nm for 100 keV $H^+$and He^+ and this corresponds to 10-20 % for ℓ=20-10 nm. A preliminary result of optical profilemeter (WYKO corp.) with the light wavelength of 651,2 nm gives that the thickness fluctuation is roughly Gaussian and $\delta\ell \approx 2$ nm for $\ell = 9$ nm, in agreement with the above value, though $\delta\ell$ increases with the film thickness ℓ for $\ell >$ 10 nm. Experimental investigation of the film uniformity is crucial.

3.5 Comparison with the Calculated ELD

The experimental energy loss distribution (ELD) of the main peak as shown in Fig. 3 or 4 is compared with the simulated ELD based on a simple model. The details of the simulation is described in ref. [13]. Slicing method as mentioned in §3.3 is employed again and let the sliced layer thickness be $\Delta\ell=\ell/n$. In each slice with thickness $\Delta\ell$, the energy loss is calculated according to the Coulomb scattering with free electrons,

$$\sigma(\Delta E) \propto 1/\Delta E^2 \text{ for } u < \Delta E < T_m \text{ and } \sigma(\Delta E) = 0 \text{ otherwise.} \qquad (8)$$

Then the energy loss spectrum in each layer is accumulated to generate the total energy loss spectrum. Here $T_m=(4m_e/m_1))E$ is the maximum energy transfer, m_e, m_1 and E being the electron mass, ion mass and the incident ion energy and u is the cut-off energy.

The results of calculation depend on the choice of u and $\Delta\ell$, but this dependence is not seriously significant [13]. In this calculation, contributions from plasmon excitation and K-shell ionization and excitation are discarded. Vavilov distribution [28] is the limiting case for u and $\Delta\ell$->0. Here, Gaussian distribution is assumed for the fluctuation of the film thickness, as mentioned in §3.4. Fig. 7 shows the comparison of the experimental ELD(o) with the calculated ELD (dashed line) with $\sigma\ell$=20 %. The calculated ELD agrees well with the experimental ELD. Inclusion of plasmon and inner shell excitations, elimination of arbitrary parameters of u and $\Delta\ell$ would be interesting and this is under way. Also shown is the Vavilov distribution with $\sigma\ell$=0 (solid line) [29], which also agrees well the experimental ELD.

It also appears that the asymmetry parameter A defined by $A=(W_2-W_1)/(W_2+Wi)$ is an useful parameter for characterizing ELD [13]. Notice that the asymmetry parameter has the relation with the higher order (3rd) moment of ELD [30].

3.6 ELD of H_2^+

The ELD of 100 kev H_2^+ was also measured [15]. The ratio of the peak energy loss of H_2^+ per proton over H^+ at the same velocity was obtained as 0.9 and slightly smaller than unity expected for the independent-particle model, as shown in Fig. 8. Also shown in Fig. 8 is the ratio of the full-width at the half maximum of H_2^+ over H+ and this was varied from 1.3-1.6 and deviate from 1.41 of the independent- particle model. This indicates that the vicinage effect on the straggling differs from that on the energy loss. The present result would be useful for further understanding of the vicinage effect.

4 Summary

Energy loss distribution (ELD) of H^+, $He^+$and H_2^+ with ~100 keV transmitted through carbon films has been measured by high resolution energy loss spectroscopy(~30 eV) in order to investigate details of the electronic energy loss process. The results are summarized as follows.

(1) No peak corresponding to plasmon excitation was observed, even though a crude estimation predicts that the intensity is comparable with that of the zero energy loss peak. Careful investigations are required both experimentally and theoretically.

(2) The zero energy loss peak was detected and the inelastic mean free path (IMFP) was deduced as 0.6 and 0.9 nm for 100 keV H^+ and He^+, respectively, taking care of the pin hole effects inferred from the transmission efficiency of H_2^+. These experimental IMFP's are somewhat larger than the calculated values

(3) The main ELD deviates significantly from the Gaussian for thin films and is compared with the ELD of simulation (Vavilov distribution etc.), including non uniformity of films. Good agreement was found between the experimental and calculated ELD. The energy loss straggling was also evaluated and agree reasonably well with those in literature.

(4) The ratio of the full-width at the half maximum of H_2^- over H^+ was varied from 1.3-1.6 and these deviate from 1.41 of the independent- particle model, indicating that the vicinage effect on the straggling differs from that on the energy loss.

The author is grateful to Dr. K. Kitoh for helpful discussions and technical assistance, to Prof. Y. Yamazaki for supplying carbon films and helpful discussions, to Dr. H. Tawara for valuable discussions, to Dr. S. Aral for electron energy loss experiment and to Dr. S. Miyagawa and Dr. M. Ikeyama for optical profilemeter experiments.

REFERENCES

1. J. F. Ziegler, J. P. Biersack and U. Littmark, "The Stopping and Ranges of Ions in Solids", (Pergamon, 1985).
2. N. Matsunami and K. Kitoh, Nucl. Insrum. & Mtth. B67(1992)50.
3. H. Raether, "Excitation of Plasmons and Interband Transitions by Electrons", (Springer, 1980).
4. N. Matsunami, Nucl. Insrum. & Meth. B115 (1996) 14.
5. M. P. Seah and W. A. Dench, Surf. Interface. Anal. 1 (1979)2.
6. N. Matsunami, Scanning Microscopy 1 (1987)1593.
7. N. Matsunami, Nucl. Insrum. & Moth. B64 (1992) 800.
8. J. R sabin and J. Oddershede, Nucl. Insrum. & Meth. B27 (1987) 280.
9. U. Sander, H. H. Bukow and H. V. Buttlar, Nucl. Insrum. & Meth. 167 (1979)35.
10. N. Matsunami, Nocl. Insrum. & Meth. B79 (1993) 549.
11. N. Matsunami, H. Hososno and M. Tazawa, Proc. Ion Beam Modification of Materials (Elsevier,1996) 999.

12. J. Robertson, Adv. in Phys. 35 (1986) 317.

13. N. Matsunami and K. Kitoh, Nucl. Insrum. & Meth. B85 (1994) 556.

14. N. Matsunami and K. Kitoh, NIFS-88(National Institute for Fusion Science, Nagoya, Japan, 1991).

15. N. Matsunami, Nucl. Insrum. & Meth. B I5 (1996) 55.

16. J. C. Ashley, J. Electron Spectrosc. Relat. Phenom. 50 (1990) 323.

17. J. C. Ashley, J. J. Cowan, R. H. Ritchie, V. E. Anderson and J. Hoelzl, Thin Solid Films 60 (1979) 361.

18. J. Lindhard, Mat. Fys. Medd. 28 no8 (1954).

19. D. R. Penn, Phys. Rev. B35 (1987) 482.

20. K. Jacobi and J. Hölzl, Surf. Sci. 26(1971)54.

21. R. G. Steinhardt, J. Hudis and M. L. Perlman, Phys. Rev. 5 (1972) 1016.

22. C. Martin, E. T. Arakawa, T. A. Callcott and J. C. Ashley, J. Electron Spectrosc.Relat. Phenom. 35 (1985) 307.

23. T. Kaneko, NIFS-DATA-9 (National Institute for Fusion Science, Nagoya, Japan, (1990).

24. N. E. Capuj, J. C. Eckardt, G. H. Lantschner, N .R. Arista and M. M. Jakas, Phys. Rev. A39 (1989) 1 049.

25. M. A. Briere and J. P. Biersack, Nucl. Instr. and Meth. B64 (1992) 693.

26. T. Kaneko and Y. Yamamura, Phys. Rev. A33 (1980) 1653 and private communication.

27. F. Besenbacher, J. U. Andersen and E. Bonderup, Nucl. Instrum. & Meth.168(1980)1.

28. P. V. Vavilov, Sov. Phys. JETP 5(1957)749.

29. Y. Kido (private communication).

30. P. Sigmund and K. B. Winterbon, Nucl. Insrum. & Meth. BI2 (1985) 1.

Table I Calculated IMFP λ_0 (nm) and stopping power dE/dx (ev/nm) for protons in carbon, using various dielectric functions [17-19]. Also included are the semi-empirical stopping powers [1]. Contribution of K- shell to stopping powers (0.5, 1.3 and 5.6 % for 25, 100 and 400 keV H$^+$ [23]) are discarded in the calculation.

	λ_0(nm)			dE/dx (ev/nm)		
Proton Enerqy (keV)	**25**	100	**400**	25	100	400
Ashley(a)	**0,8**	0,4	0,88	18	110	68
Lindhard (b)	**0,25**	0,13	0,54	100	200	90
Penn (c)	**0,33**	0,33	0,8	48	110	64
ZBL				129	**152**	90

Dielectric functions used in this calculation denoted by (a), (b) and (c) are taken after refs. [17], [18] and [19].

Figure captions

Fig. 1 A schematics of the high-resolution ion energy loss spectrometer (after ref/[6]). The bottom figure shows the details of deflector in the scattering chamber and sample assembly.

Fig. 2 Energy loss spectrum for 200 keV electrons transmitted through 21 nm carbon film. The resolution was ~1 eV. A peak at 24 eV is due to plasmon excitation, from which the density of carbon film was determined. A peak around 300 eV is due to K-shell ionization.

Fig. 3 Energy loss spectrum for 100 and 120 keV H^+ transmitted through a carbon film with thickness of ℓ6.6 nm (after ref. [2]). The main energy loss peak is seen around 1 keV and a peculiar peak is also seen around 210 eV. The solid line is the Gaussian or asymmetric- Gaussian fit to the data. Notice that the horizontal scale is different for two peaks and 1/25 means that the yield of $\Delta E=0$ to 300 eV including the peculiar peak is smaller by 25 than that of the main energy loss peak. The vertical arrows around the main energy loss peak indicate the mean energy losses. Notice that no plasmon peak was seen around 25 eV. See Fig. 4 for the details of the zero energy loss peak.

Fig. 4 Energy loss spectrum for 100 keV H^+ transmitted through a carbon film with thickness ℓ of 6.4 nm, showing the main energy loss peak around 1 keV and the zero energy loss peak (after ref. [4]). The solid line is the asymmetric-Gaussian fit to the main peak. Notice that the horizontal scale is different for two peaks and x2200 means that the yield around $\Delta E=0$ is smaller by 2200 than that of the main energy loss peak. The vertical arrows around the main energy loss peak indicate the mean energy loss. Crosses are the zero energy loss peak for 100 keV H_2^+, which originates predominantly transmission through pinholes and should be subtracted to obtain the true zero energy loss peak for 100 keV H^+.

Fig. 5 Energy dependence of inelastic mean free path; present results for H^+ (o) and He^+ (Δ), calculated results for positrons (solid line) and electrons (dashed line)[16]. E and E_e are the energies of H^+, He^+ (per nucleon) and electron (or positron) having the same velocities. The dot-dashed and double dot-dashed lines show the calculated result for electrons including extension to low energies and protons, respectively, without the exchange effect after ref.[17]. The calculated values using the dielectric functions [18] and [19] are also shown by (– – - - – – ; Lindhard) and (– – - – – ; Penn). Experimental data source: Δ= ref. 20; x = ref. 21; + = ref. 22.

Fig. 6 Comparison of the experimental energy loss distribution (ELD) shown by open circles with the calculated ELD for 100 keV H^+ transmitted through carbon film with thickness of 10 nm. The dashed line is the calculated ELD with the variance of the film thickness $\delta\ell$=20 %, using a simple method (see §3.5). The solid line is the Vavilov distribution calculated by Y. Kido with $\delta\ell$=0 [27].

Fig. 7 Ratio of the energy loss of 100 keV H_2^+ per proton divided that of 50 keV H^+ (o) and ratio of full width at half maximum of 100 keV H_2^+ divided by that 50 keV H^+ (x) (after ref. [15]).

HIGH RESOLUTION SPECTROMETER

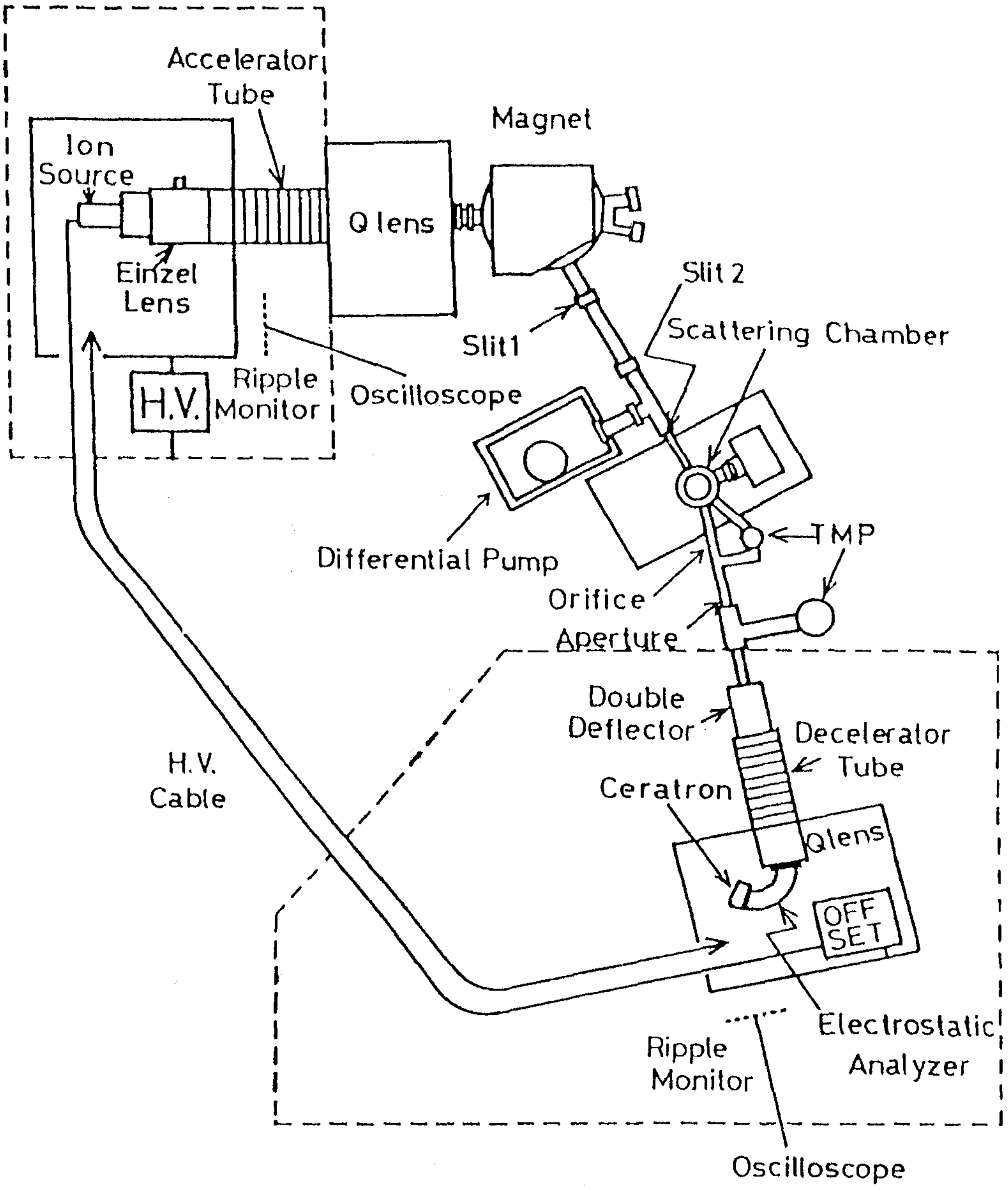

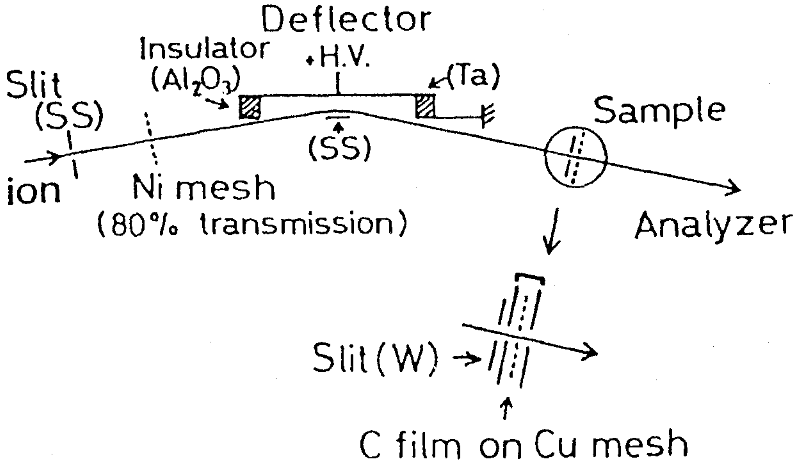

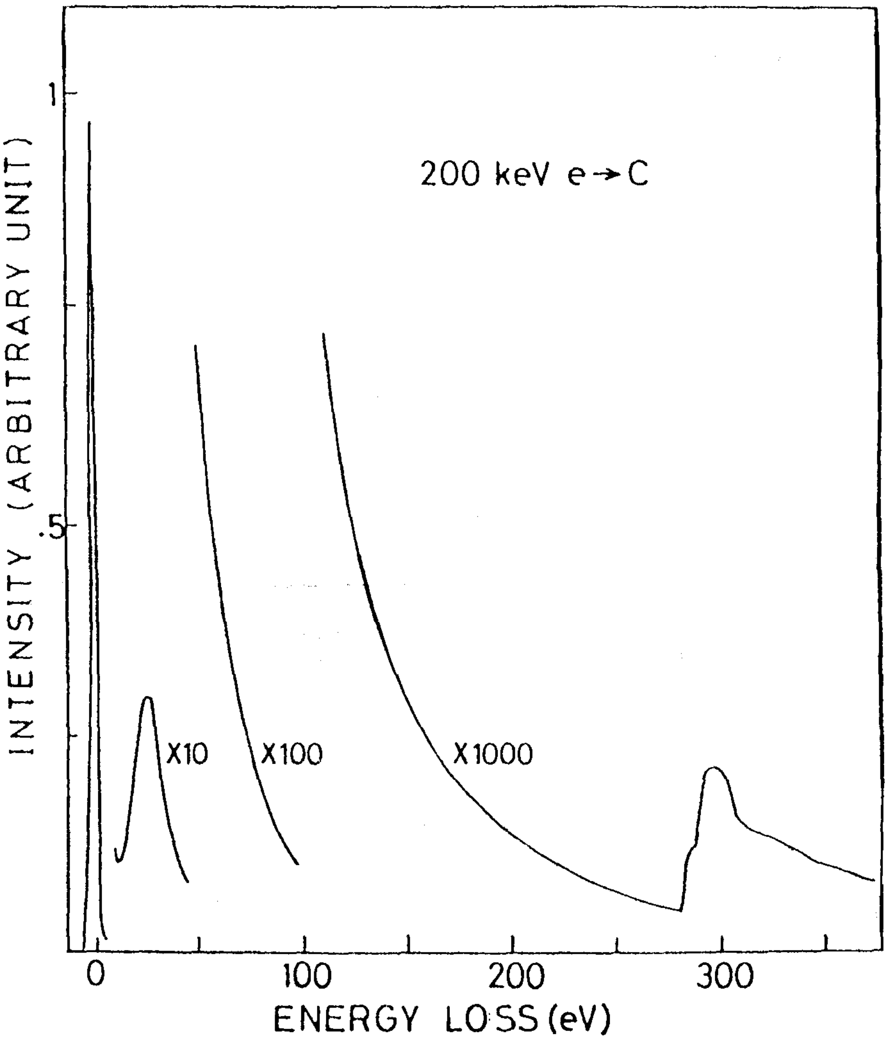
200 keV e → C
INTENSITY (ARBITRARY UNIT)
1
.5
X10
X100
X1000
0
100
200
300
ENERGY LOSS (eV)

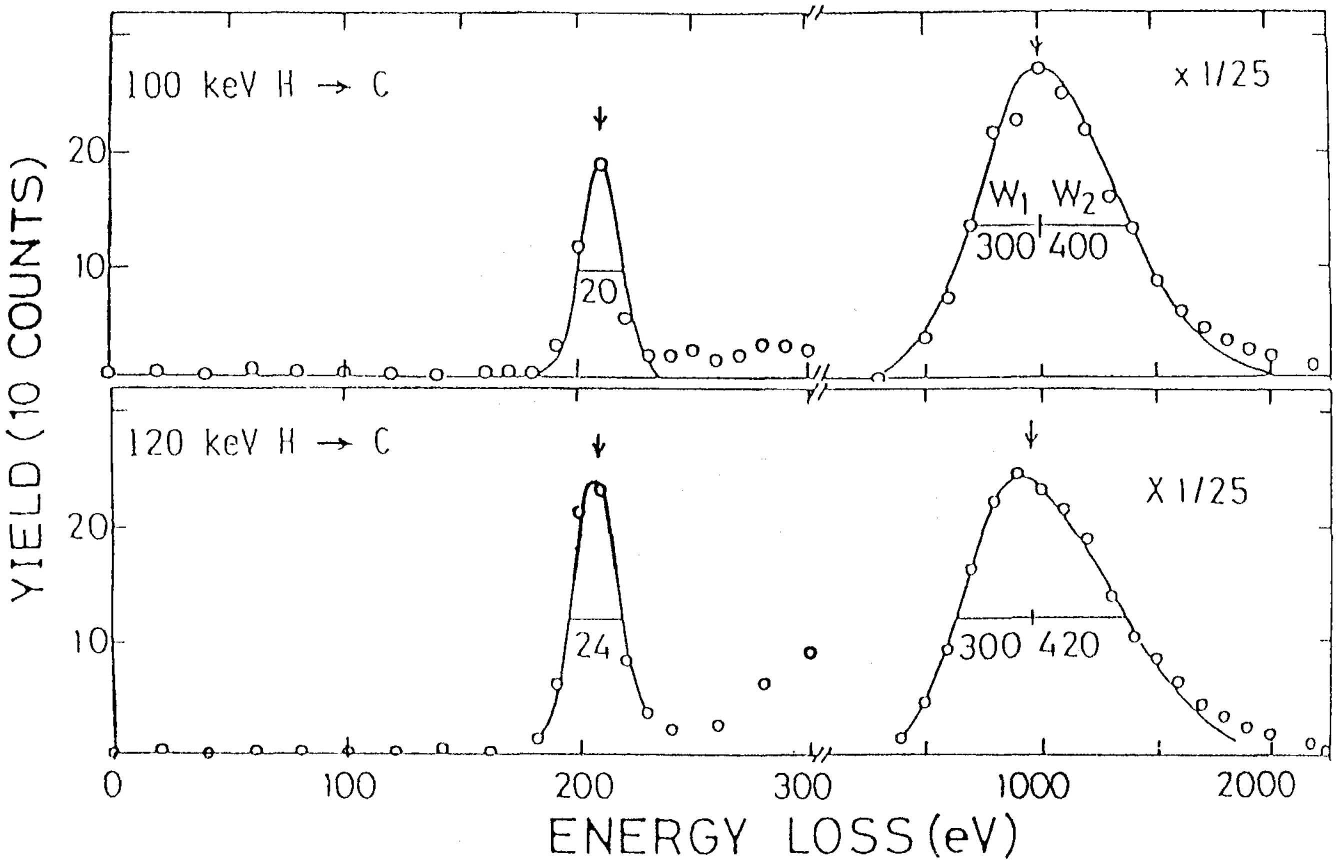
100 keV H → C
x 1/25
20
W1
W2
300
400
120 keV H → C
X 1/25
24
300
420
YIELD (10 COUNTS)
20
10
0
100
200
300
1000
2000
ENERGY LOSS (eV)

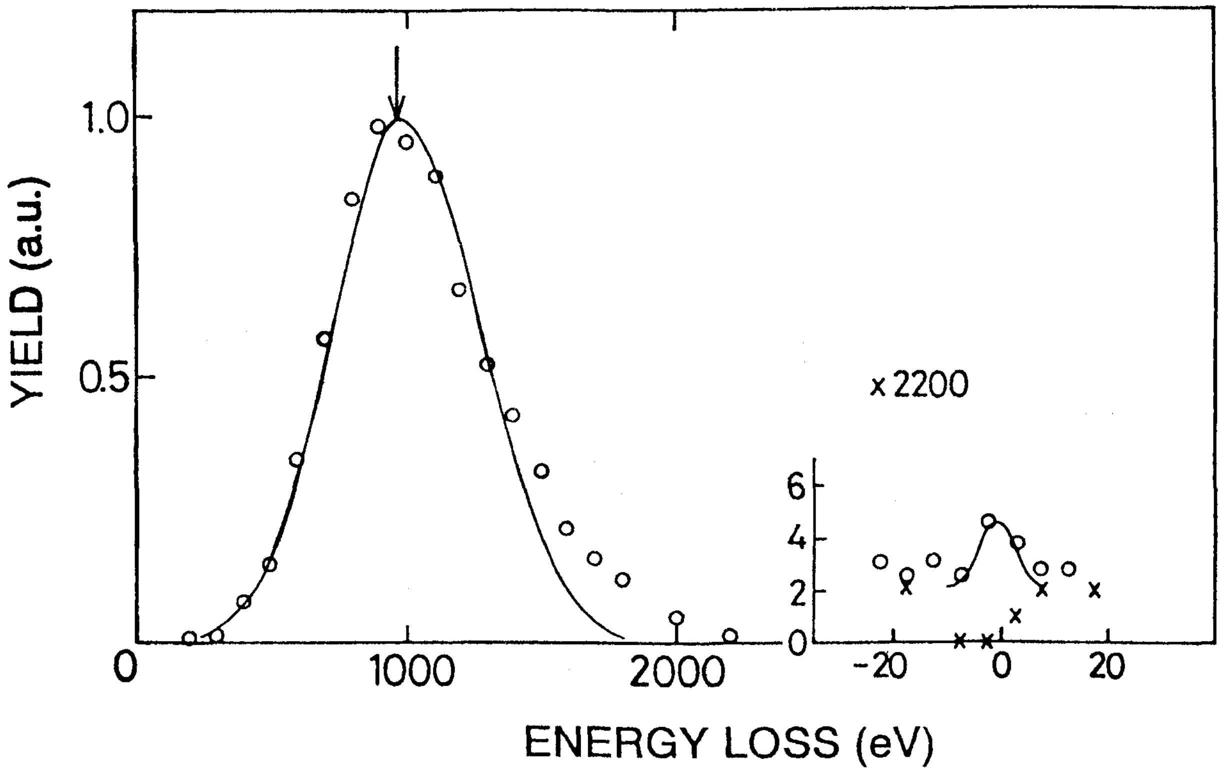
YIELD (a.u.)
1.0
0.5
x 2200
6
4
2
0
-20
0
20
0
1000
2000
ENERGY LOSS (eV)

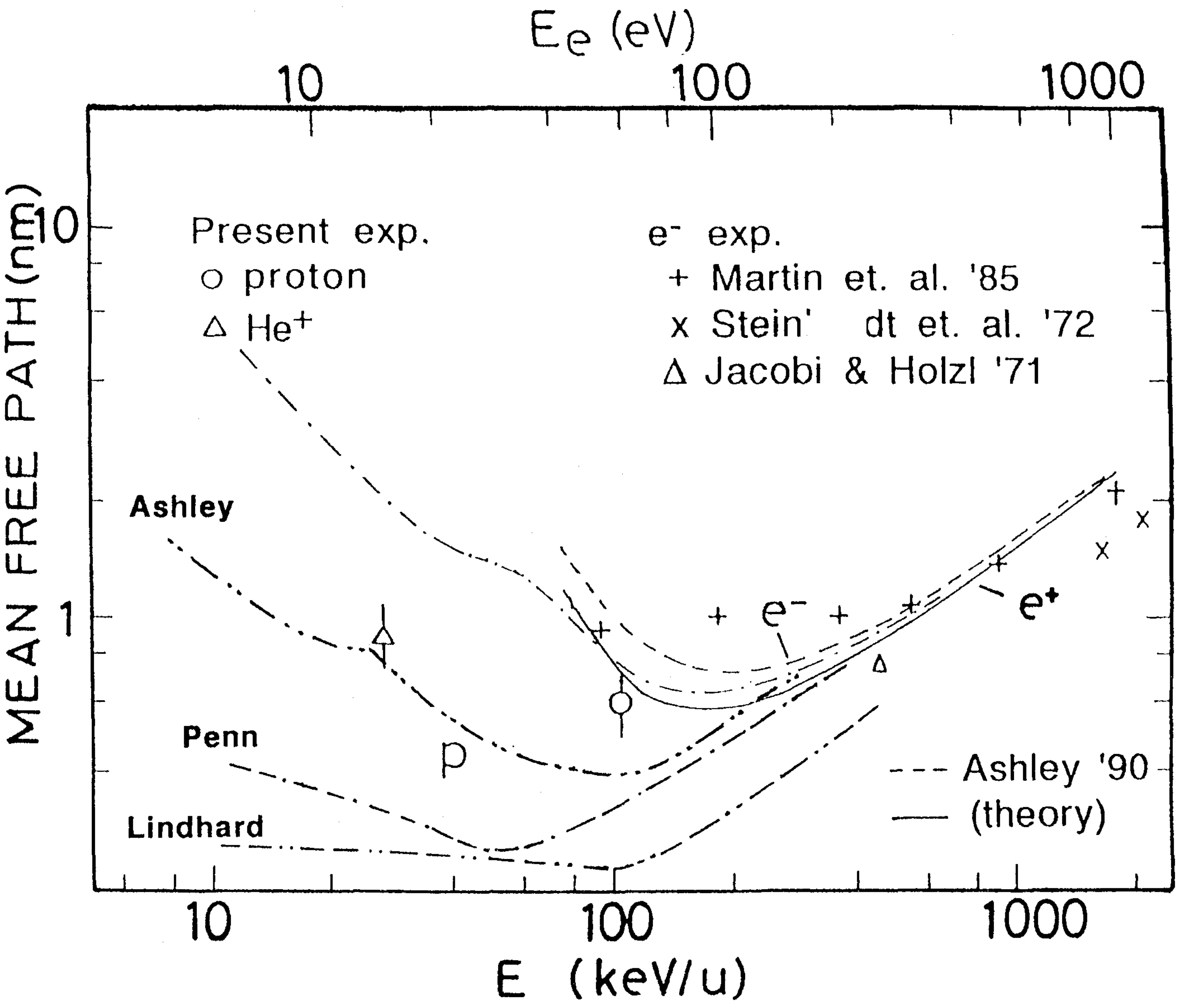Ee (eV)
10
100
1000
MEAN FREE PATH (nm)
10
1
Present exp.
○ proton
△ He+
e- exp.
+ Martin et. al. '85
x Stein' dt et. al. '72
△ Jacobi & Holzl '71
Ashley
Penn
Lindhard
p
e-
e+
--- Ashley '90
— (theory)
10
100
1000
E (keV/u)

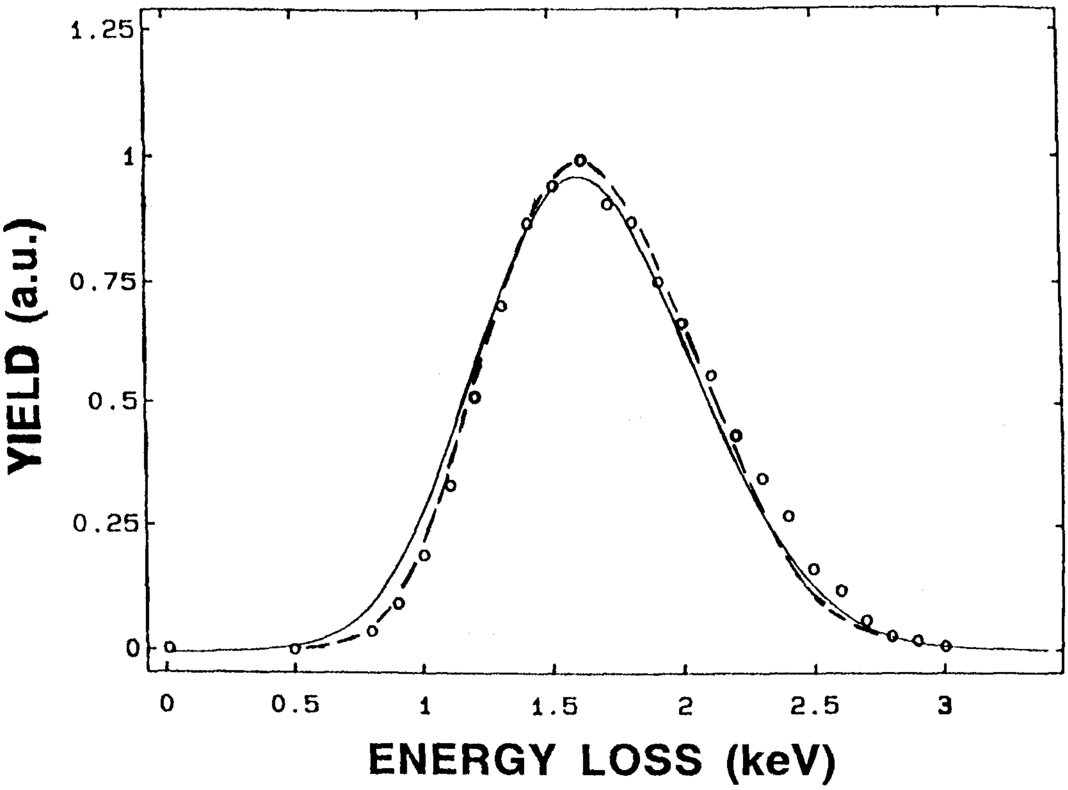
YIELD (a.u.)
1.25
1
0.75
0.5
0.25
0
0
0.5
1
1.5
2
2.5
3
ENERGY LOSS (keV)

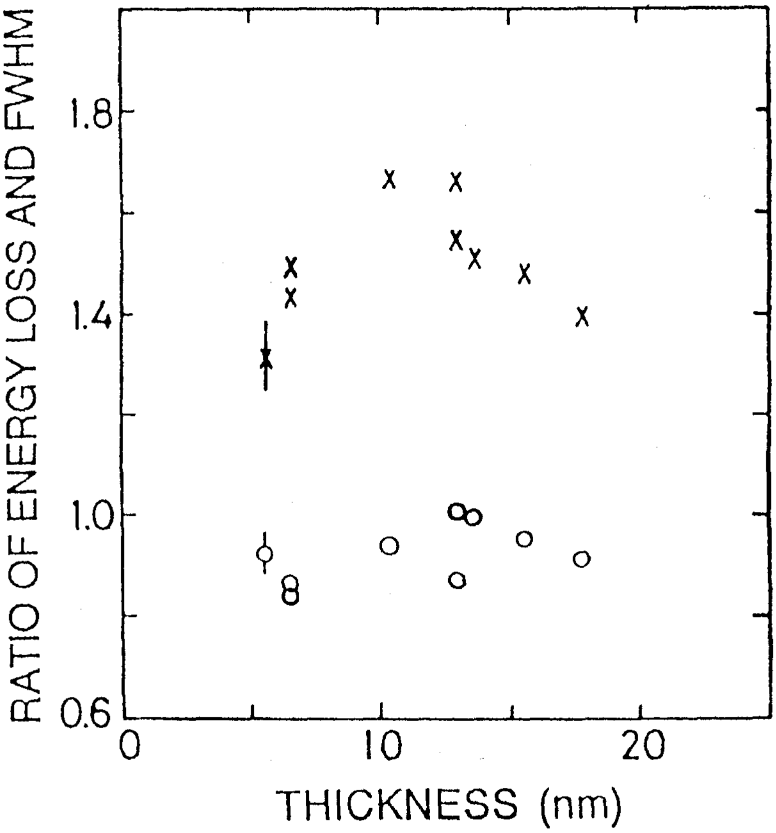
RATIO OF ENERGY LOSS AND FWHM
1.8
1.4
1.0
0.6
0
10
20
THICKNESS (nm)